Molecular Therapy
Oncology
Original Article

FOS$^+$ B cells: Key mediators of immunotherapy resistance in diverse cancer types

Xiangyang Zhang,[1,2] Jiayao Ma,[1] Yihong Chen,[1] Xiangying Deng,[1] Yan Zhang,[3] Ying Han,[1] Jun Tan,[4] Gongping Deng,[5] Yanhong Ouyang,[5] Yulai Zhou,[1] Changjing Cai,[1,6] Shan Zeng,[1,6] and Hong Shen[1,6]

[1]Department of Oncology, Xiangya Hospital, Central South University, Changsha 410008, Hunan, China; [2]Department of Biomedical Sciences, City University of Hong Kong, Hong Kong 518057, China; [3]Department of Oncology, Yueyang People's Hospital, Yueyang Hospital Affiliated to Hunan Normal University, Yueyang 414022, Hunan, China; [4]Department of Neurosurgery, Xiangya Hospital, Central South University, Changsha 410008, China; [5]Department of Emergency, Hainan General Hospital, Hainan Affiliated Hospital of Hainan Medical University, Haikou, 570311 China; [6]National Clinical Research Center for Geriatric Disorders, Xiangya Hospital, Central South University, Changsha, 410008 China

While immunotherapy has marked significant advances in cancer treatment, resistance remains a challenge. The complexity of the tumor microenvironment, particularly the role of B cell subpopulations, is a critical factor affecting treatment efficacy. In this study, we conducted analyses of single-cell RNA sequencing data from immunotherapy patients (n = 25) to explore the biomarker of immunotherapy resistance. Spatial transcriptome analysis, immunofluorescence analysis, and multi-cancer immunotherapy transcriptome analysis (n = 1,253) were used to validate our finding, and the potential mechanisms were explored. FOS$^+$ B cells, identified across multiple cancer types, were associated with poor response to immunotherapy. FOS may form AP-1 (activator protein 1) with JUNB, thereby promoting the expression of Blimp-1 and subsequently facilitating the differentiation of B cells into immunosuppressive plasma cells. Furthermore, FOS$^+$ B cells were linked to altered tumor necrosis factor signaling pathways, suggesting a mechanism for their immunosuppressive effects. Our findings highlight FOS$^+$ B cells as important players in immunotherapy resistance, providing a novel biomarker for predicting treatment response. This study not only deepens our understanding of the immunological landscape influencing immunotherapy efficacy but also opens avenues for targeted interventions to overcome resistance.

INTRODUCTION

Immunotherapy, including immune checkpoint inhibitors (ICIs), has shown excellent performance as a landmark malignancy treatment in a variety of cancers, including lung cancer,[1] colorectal cancer,[2] and skin tumors.[3] However, not all patients benefit from immunotherapy, and many patients develop immunotherapy resistance.[4] Although there are many studies on immunotherapy resistance, the mechanism behind it remains unclear, presenting a substantial challenge in the selection of appropriate treatment regimens.

Previous studies have shown that the heterogeneity of the tumor microenvironment may be an important reason for the different efficacies of immunotherapy in patients.[5–7] Immune cells, as an important component of the tumor microenvironment, play an important role in anti-tumor immunity and thus affect immunotherapy efficacy and patient prognosis.[8] The influence of immune cells on the effect of immunotherapy has been well recognized.[9] Many previous studies have shown that immune cells, such as B cells, have positive implications for immunotherapy,[10–12] but a few studies showed that B cells affect immunotherapy efficacy.[13,14] Therefore, we speculate that a certain group of B cells has a negative effect on immunotherapy, while the other B cells promote immunotherapy efficacy, and further studies are needed to prove this conjecture and to investigate which B cells reduce immunotherapy efficacy.

Single-cell RNA sequencing (scRNA-seq) can be used to measure RNA expression levels at the cellular level.[15] scRNA-seq, combined with a variety of cell-specific markers, enables the identification of cell types, cell functional status, levels of cell-to-cell interactions, and the differentiation status using several analysis methods.[16] With the advancement of technologies such as single-cell sequencing, our understanding of B cell subpopulations and their impact on the immune microenvironment has deepened. Various B cell subgroups, including naive B cells and memory B cells, have been associated with favorable prognoses in malignant tumor patients. Conversely, regulatory B cells (Bregs) have been linked to poorer prognoses as they secrete multiple immunosuppressive cytokines, including IL-10, IL-35, and TGF-β.[10,17] However, the precise role and mechanisms by which B cells operate in immunotherapy warrant further investigation, necessitating continued research in this area.

We analyzed single-cell sequencing data from immunotherapy patients to perform a comparative analysis of tumor-infiltrating B cells to obtain immunotherapy-related B cells and their marker genes. We discovered that FOS$^+$ B cells negatively affect immunotherapy

Received 16 July 2024; accepted 16 October 2024;
https://doi.org/10.1016/j.omton.2024.200895.

Correspondence: Hong Shen, Department of Oncology, Xiangya Hospital, Central South University, Changsha 410008, Hunan, China.
E-mail: hongshen2000@csu.edu.cn

outcomes, in contrast to other B cell subtypes across four cancer types. Immunofluorescence analysis and pan-cancer immunotherapy cohort analysis also indicated that FOS^+ B cells negatively relate to immunotherapy efficiency and anti-tumor immunity. Furthermore, we explored the possible mechanisms underlying the effect of FOS^+ B cells. This study sheds light on the imaging of B cells for immunotherapy and provides directions and ideas for overcoming drug resistance in immunotherapy (Figure 1).

RESULTS

FOS^+ B cells are associated with immunotherapy response

We first analyzed a single-cell dataset of basal or squamous cell carcinoma (BCC) (GSE123813) of 10 immunotherapy patients, 6 of whom responded to immunotherapy (R) and 4 of whom did not respond to immunotherapy (NR). A total of 40,314 immune cells were included in this dataset, which were clustered by PCA downscaling and displayed by UMAP as shown in Figure 2A and divided into 12 subgroups, of which the number of cells in groups 2, 6, and 10 was statistically different between R and NR patient groups ($p < 0.001$, Figures 2B and 2C). The marker genes of each cell group are shown in Figure 2D. To define the types of each subgroup of cells, we analyzed the expression of immune cell marker genes among the 12 cell types (Figure 2E). CD19, CD79A, and MS4A1 were defined as B cell marker genes. IGHG1, MZB1, SDC1, and CD79A were defined as plasma cell marker genes. CD68, CD163, and CD14 were defined as macrophage and monocyte marker genes. CD3D, CD3E, CD8A, and CD4 were defined as T cell marker genes. FGFBP2, FCG3RA, and CX3CR1 were defined as NK cell marker genes. Based on these gene expressions, we defined cluster 2 cells as B cells, cluster 10 cells as plasma cells, and cluster 6 cells as monocytes or macrophages (Figure 2F). As shown in Figure 2G, CD19, CD79A, and MS4A1 were characteristically expressed in cluster 2 cells, which were defined as B cells.

We further clustered the 5,969 B cells in descending order into 4 groups (Figure S1A), and the third group ($n = 269$) showed a significant quantitative difference between the R and NR groups ($p < 0.0001$) and was enriched in NR patients (Figures S1B and S1C). Marker genes in each group of B cells are shown in Figure S1D. The five genes with the highest specific expression in group 3 B cells were FOS, FOSB, SLC2A3, NR4A2, and JUNB, and FOS has the highest degree of differential expression ($p < 0.0001$, $\log_2FC = 1.5335$, Figures S1G–S1K). Therefore, we defined the third group of B cells as FOS^+ B cells and performed subsequent analyses on them. Subsequently, we conducted an analysis of the correlation between FOS^+ B cells and immunotherapy in patients with colon cancer, lung cancer, and liver cancer.

To further substantiate our finding, we collected surgical specimens from two colon cancer patients (one showing no response to the treatment and the other exhibiting a partial response) and one hepatocellular carcinoma (HCC) patient (evaluated as stable disease) who underwent neoadjuvant immunotherapy at Xiangya Hospital, Central South University, and conducted single-cell sequencing. We performed dimensionality reduction and clustering on this single-cell data, dividing 12,484 cells into 13 subgroups (Figures S2A and S2B). The cells in the 7th subgroup exhibited specific expression of B cell markers, MS4A1, and CD79A (Figure S2C). Subsequently, we further clustered B cell subgroups into 5 clusters (Figure S2D). Notably, clusters 0 and 2 of B cells predominantly resided in samples from immunotherapy non-responders, with cluster 0 B cells showing larger differences between NR and R patients ($n = 190$, Figures S2E and S2F). It is worth noting that FOS was among the top 5 marker genes for cluster 0 B cells ($p = 5.61e{-}18$, $\log_2FC = 1.5153$, Figure S2G). FOS also showed significant differences in expression among the 5 B cell clusters ($p = 3.8 \times 10^{-11}$, Figure S2H) as well as between different patients ($p < 2.2 \times 10^{-16}$, Figure S2I). Single-cell data from a HCC patient who received immunotherapy were also analyzed. Among the 14 cell subgroups (Figure S3A), we defined the 8th group as B cells (Figure S3B). Further analysis revealed that B cells expressing the FOS gene were scarce. We examined four previously identified immunosuppressive B cell markers (Figures S3D–S3L), and TGF-β expression showed significant differences in B cells from lung cancer, BCC, and colon cancer ($p = 7 \times 10^{-8}$ to 0.015), whereas IL-10, IL-35, and CD21 showed no significant differences.

We similarly analyzed a dataset comprising single-cell data from 12 non-small cell lung cancer patients who received immunotherapy (Figure S2J). We defined the third group of cells as B cells (Figure S2K) and further clustered B cells into six classes (Figures S2L and S2M). We found that B cells in immunotherapy NRs exhibited significantly higher expression of FOS ($p < 2.2 \times 10^{-16}$) and JUNB ($p < 2.2 \times 10^{-16}$) compared with responders (Figures S2N and S2O), with cluster 0 cells showing FOSB, a member of the FOS family, as a top 5 marker gene (Figure S2P). In addition, the expression of the two genes is highly positively correlated (Figures S1E and S1F).

Through the analysis of colorectal cancer spatial transcriptome data and their corresponding single-cell data, we observed a significant reduction in the infiltration levels of T cells and $CD8^+$ T cells in samples with high FOS^+ B cell infiltration (Figures 3A and 3B). To further substantiate the correlation between FOS^+ B cells and immunotherapy resistance, we performed multi-immunofluorescence testing on samples from eight colon cancer immunotherapy patients, including four Rs and four NRs. We observed a significant decrease of FOS^+ B cells in samples from immunotherapy Rs (Figure 3C), and the difference in the proportion of B cells among the total B cells between the two groups of patients was statistically significant ($p = 0.013$, Figure 3D). The analysis based on single-cell data from immunotherapy patients and the results of immunofluorescence testing illustrate the correlation between FOS^+ B cells and immunotherapy resistance.

FOS may promote the differentiation of B cells into immunosuppressive plasma cells, exerting immunosuppressive effects

Our study revealed a correlation between FOS^+ B cells and immunotherapy resistance. It is noteworthy that FOS^+ B cells also use JUNB as

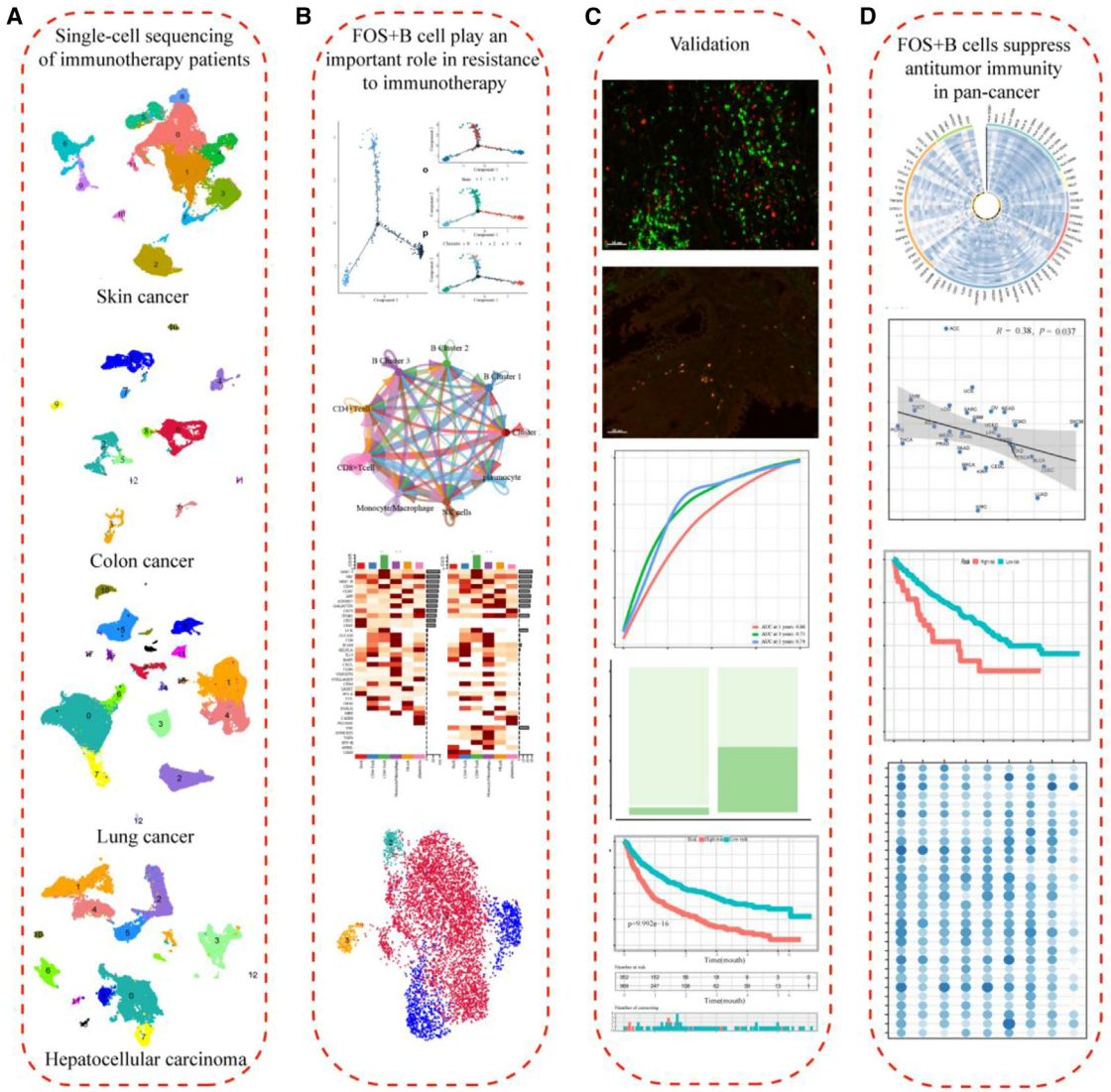

Figure 1. The flowchart of this study

(A) Through the analysis of single-cell sequencing data from skin cancer, colon cancer, lung cancer, and hepatocellular carcinoma, we have identified a significant correlation between FOS$^+$ B cells and resistance to immunotherapy. (B) We conducted investigations into the potential mechanisms by which FOS$^+$ B cells exert their influence. (C) To validate these findings, we performed immunofluorescence assays and examined transcriptomic data from a pan-cancer immunotherapy cohort. (D) Furthermore, analysis of pan-cancer transcriptomic data from TCGA suggests a potential role for FOS$^+$ B cells in suppressing pan-cancer immune functions.

a marker, and the FOS family proteins can form a transcription factor complex, AP-1, along with JUN family proteins, to function. Previous research has indicated[18] that AP-1 can facilitate the expression of B lymphocyte-induced maturation protein 1 (Blimp1) in B cells, thereby promoting the transformation of B cells into plasma cells. Thus, we hypothesized that AP-1 in B cells might promote the differentiation of B cells into immunosuppressive plasma cells by facilitating Blimp1 production.

Therefore, we analyzed the differential expression of Blimp1 in B cells from two groups of patients. In both BCC and lung cancer immunotherapy-resistant patients, the expression of Blimp1 in B cells was indeed higher than in immunotherapy Rs (Figures S4A, S4E, and S4I). Although previous studies have mostly suggested that plasma cells play a positive role in anti-tumor immunity, some research has also indicated that the presence of immunosuppressive plasma cells can hinder anti-tumor immunity. These immunosuppressive plasma cells exhibit high expression levels of IgA, PD-L1, and IL-10.[19] Consequently, we further analyzed plasma cells in both the R and NR groups. We found that in all three types of cancer, NR group plasma cells expressed higher levels of IgA compared with the R group (Figures S4A–S4L). These results

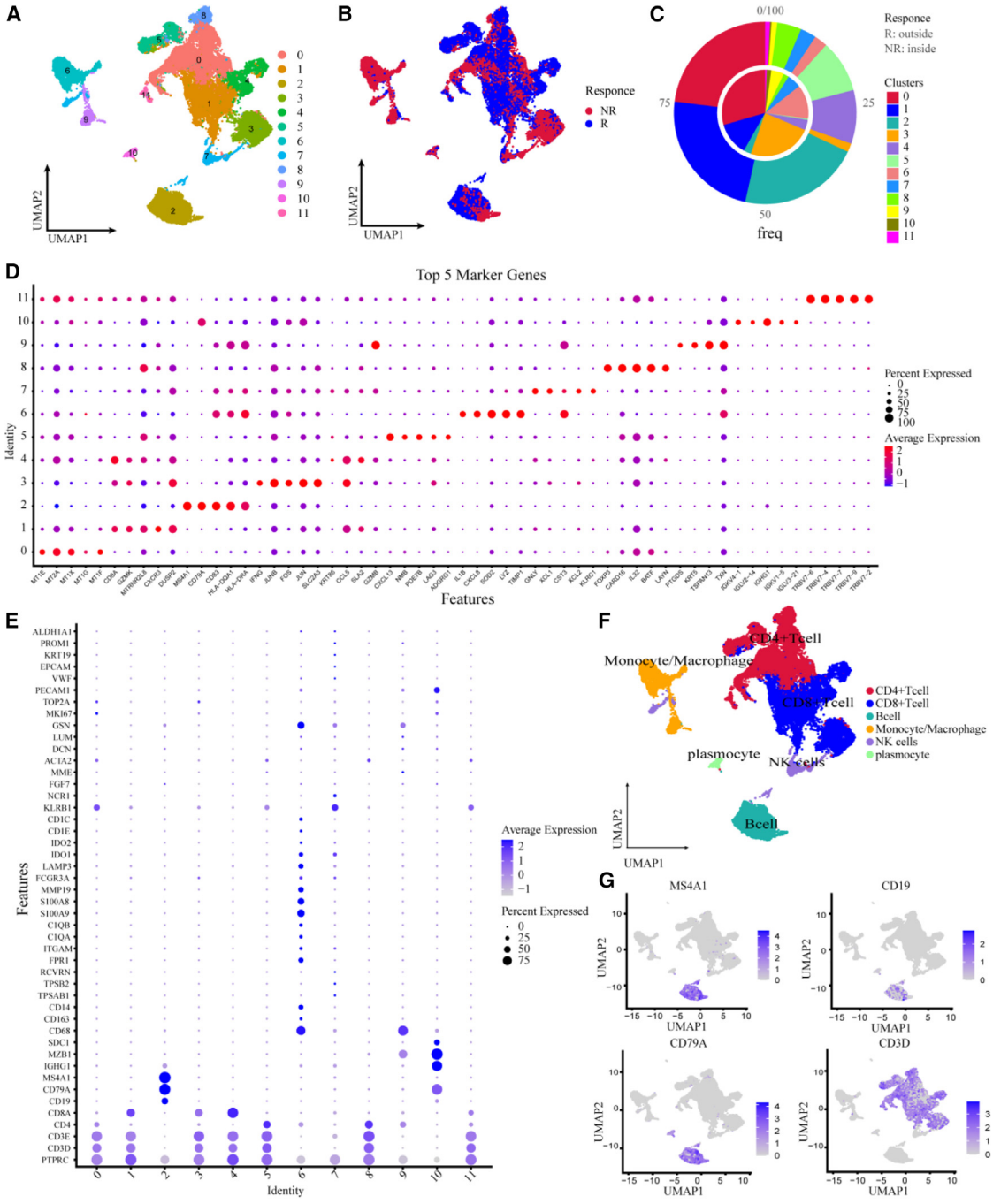

Figure 2. FOS$^+$ B cells are associated with immunotherapy resistance

(A) The cells were divided into 12 subgroups using the UMAP method for descending clustering. (B and C) The distribution of each group of cells in the R versus NR groups and the difference in the proportion of cells in each group in the R versus NR groups are shown. (D) The expression of top 5 marker genes in each cell group. (E) The expression of each cell group for immune cell marker genes. (F and G) The cells of each group were defined according to the expression of immune cell marker genes.

suggest that FOS may combine with JUNB and other JUN family proteins to form the transcription factor AP-1, thereby promoting the differentiation of B cells into immunosuppressive plasma cells (Figure 3E).

FOS$^+$ B cells exhibited greater maturity compared with other B cell subtypes

To investigate the effect of differentiation stages of B cells on immunotherapy, we performed a pseudotime analysis of 5,969 B cells. As

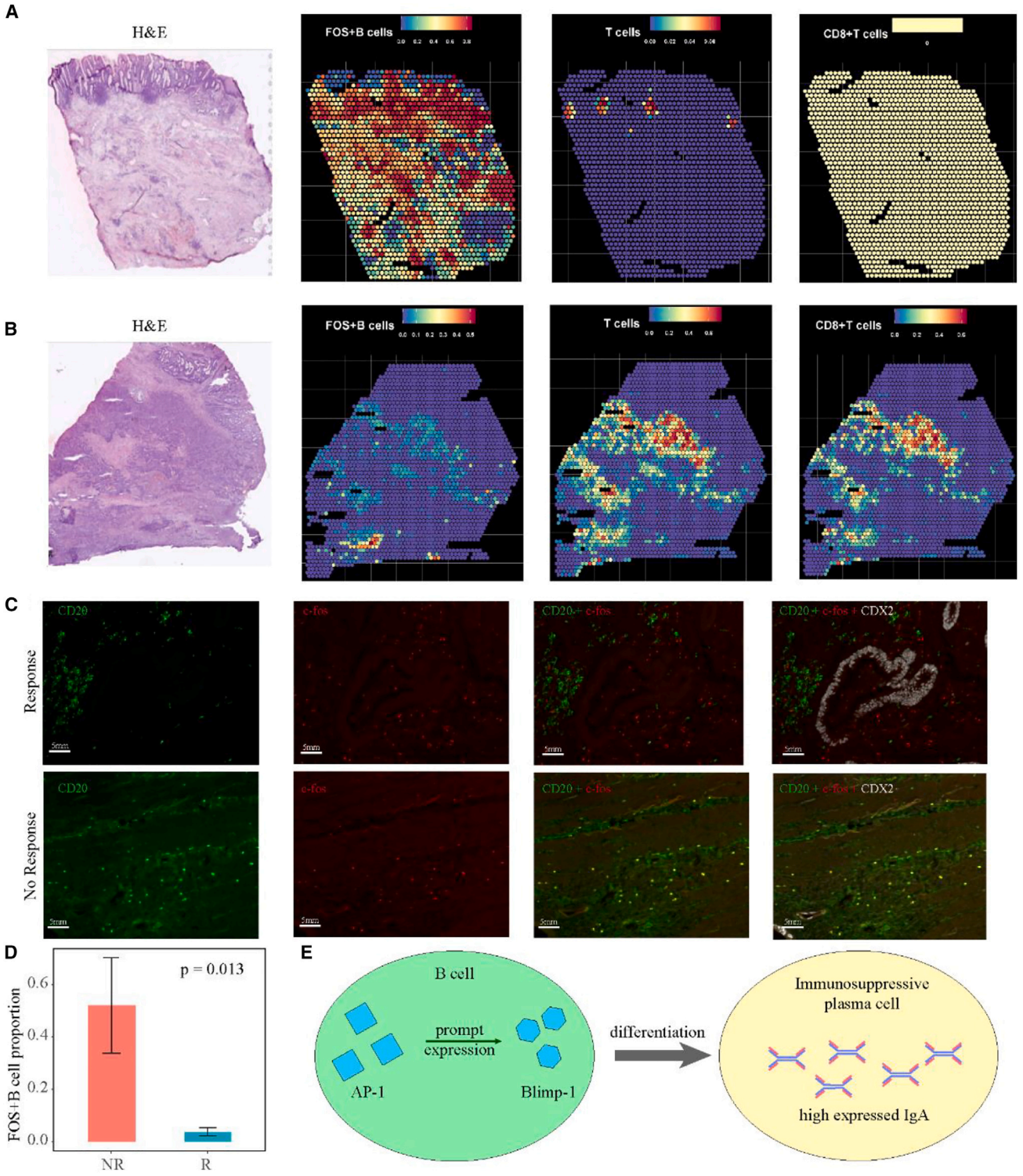

Figure 3. Validation of the relationship between FOS$^+$ B cell and anti-tumor immune

(A and B) Spatial transcriptome analysis indicates that samples with higher FOS$^+$ B cell infiltration (A) exhibit reduced infiltration of T cells and CD8$^+$ T cells compared with samples with lower FOS$^+$ B cell infiltration (B). (C) Immunofluorescence results. Immunofluorescence assays were conducted on specimens from eight colorectal cancer patients undergoing immunotherapy. The upper row displays results from responsive patients, while the lower row shows results from non-responsive patients. The

(legend continued on next page)

shown in Figure 4A, light blue represents more mature B cells, while dark blue represents more naive B cells. The NR group of B cells mostly consisted of more mature B cells (Figure 4B). According to the results of the proposed time series analysis, B cells can be divided into 11 categories, among which NR cells are mainly clustered in group 9 cells (Figures 4B and 4C). The four B cell types we obtained previously were also basically in different differentiation time periods (Figure 4D). We then used heatmaps to show the relationship between the proposed temporal subpopulation, cell type, immunotherapy response grouping, gene expression, and differentiation time, and we could see that all these factors were significantly correlated with cell differentiation time (Figure 4E).

Subsequently, we employed heatmaps to illustrate the relationships between pseudotime subgroups, cell types, immunotherapy response groups, gene expression, and differentiation time. It is evident that all these factors are significantly correlated with pseudotime. Furthermore, we observed differential expression of FOS at various stages of B cell differentiation, with high expression in mature B cells, or what we refer to as the third group of B cells (Figures 4F and 4G). IGHD and IGHM were closely associated with the degree of B cell differentiation, with higher expression levels in highly differentiated B cells. Through pseudotime analysis, we found elevated expression levels of IGHD and IGHM in B cells from the NR group (Figure 4G). In addition, we noted that TGFB1 expression increased with B cell differentiation, while IL-10 remained relatively unchanged, and IL-35 exhibited a declining trend (Figure 4G). These results collectively indicate that FOS^+ B cells tend to be more mature in terms of differentiation and are associated with resistance to immunotherapy.

FOS^+ B cells may inhibit anti-tumor immunity through TNF signaling pathway

To investigate the effect of B cells on anti-tumor immunity, we performed CellChat analysis on B cells from both R and NR groups. The four types of B cells have close cellular interactions with other types of immune cells, especially $CD8^+$ T cells (Figures 5E, 5F, 5H, and 5I). We then compared the number of signal communication between the two groups. Compared with cells in the R group, B cells in the NR group delivered more signals to $CD4^+$ T cells and monocytes/macrophages and fewer signals to $CD8^+$ T cells, NK cells, and plasma cells; B cells in the NR group received fewer signals from $CD4^+$ T cells, $CD8^+$ T cells, plasma cells, and B cells themselves, and received a higher number of signals from NK cells (Figures 5A and 5C). We also compared the strength of communication between the two groups to the cells in the R group. The B cells in the NR group sent weaker signals to the other five cells, received weaker signals from $CD4^+$ T cells, $CD8^+$ T cells, NK cells, plasma cells, and the B cells, and received stronger signals from monocytes/macrophages (Figures 5B and 5C). Finally, we compared the differences of some major signaling pathways between R and NR group immune cells and discovered that CD70 and IL-6 signaling pathways were significantly higher in R group B cells and the CD80 signaling pathway was significantly higher in NR group B cells as well as cluster 3 B cells (Figures 5D and 5G).

To compare the differences in communication between the four classes of B cells and other immune cells, we performed cell analysis again after dividing the B cells into four classes. The number and strength of communication between various immune cells are shown in Figures 6E and 6F. Compared with the other three types of B cells, FOS^+ B cells expressed fewer CD45 and CD22 signaling pathways and more tumor necrosis factor (TNF) signaling pathways. The number and strength of communications from the four types of B cells to various other immune cells are shown in Figures 6H and 6I. It can be found that the number and strength of signals from FOS^+ B cells to $CD8^+$ T cells were higher than those from other immune cells. We then further analyzed the CD22, CD45, and TNF pathways, and found that CD22 signals were mainly emitted by three other B cells besides FOS^+ B cells, acting on various immune cells, including FOS^+ B cells, with stronger effects on $CD8^+$ T cells, whose main ligand receptors were CD22 and PTPRC (Figures S5A–S5C). TNF signals are mainly emitted by FOS^+ B cells and act mainly on monocytes/macrophages, $CD4^+$ T cells, $CD8^+$ T cells, and NK cells, with TNF and TNFRSF1B as the main ligand receptors (Figures S5G–S5I).

FOS^+ B cells correlate with immunotherapy efficacy and patient's prognosis in pan-cancer

To assess the level of infiltration of FOS^+ B cells at the genetic level, we intersected 563 B cell marker genes with FOS^+ B cells differently expressed genes, and obtain 170 genes (Figure 6A), which were analyzed by PCA and Lasso regression to obtain 15 genes, namely SWAP70, POU2F2, TEX9, AIM2, LGALS1, KLHL6, PSMB9, HSPE1, IGHMBP2, HLA.DQA2, HMGN2, SRFBP1, ZRANB2, CYB5A, and TAF7. To explore the correlation and predictive role of FOS^+ B cells with immunotherapy efficacy and patient prognosis, we developed a predictive model using these 15 genes. We divided a fused immunotherapy transcriptome dataset into the training set ($n = 721$) and validation set 1 ($n = 154$). The model achieved excellent results in this fusion dataset (Figures 6G–6I), with an area under the curve (AUC) of 0.75 for 3-year overall survival (OS) and 0.74 for 5-year OS, and the prognosis of patients in the high- and low-risk groups differed significantly ($p < 0.0001$), as did the efficacy of patients in the two groups ($p = 0.0310$).

We then validated the model in four immunotherapy cohorts. We performed model validation in the Xiangya HCC immunotherapy cohort ($n = 36$), with an AUC of 0.78 for 1-year progression-free survival (PFS), AUC of 0.98 for 5-year PFS, AUC of 1 for 1-year OS, AUC of 0.72 for 3-year OS (Figures 6B and 6D). Patients with low-risk scores had better outcomes than patients with high-risk scores

expression of CD20, c-fos, and CDX2 were measured. (D) Statistical analysis of the immunofluorescence results suggests a significant enrichment of FOS^+ B cells in specimens from patients who exhibited immunotherapy resistance. (E) FOS may form a transcription factor AP-1 with JUNB, thereby promoting the expression of Blimp-1 and subsequently facilitating the differentiation of B cells into immunosuppressive plasma cells.

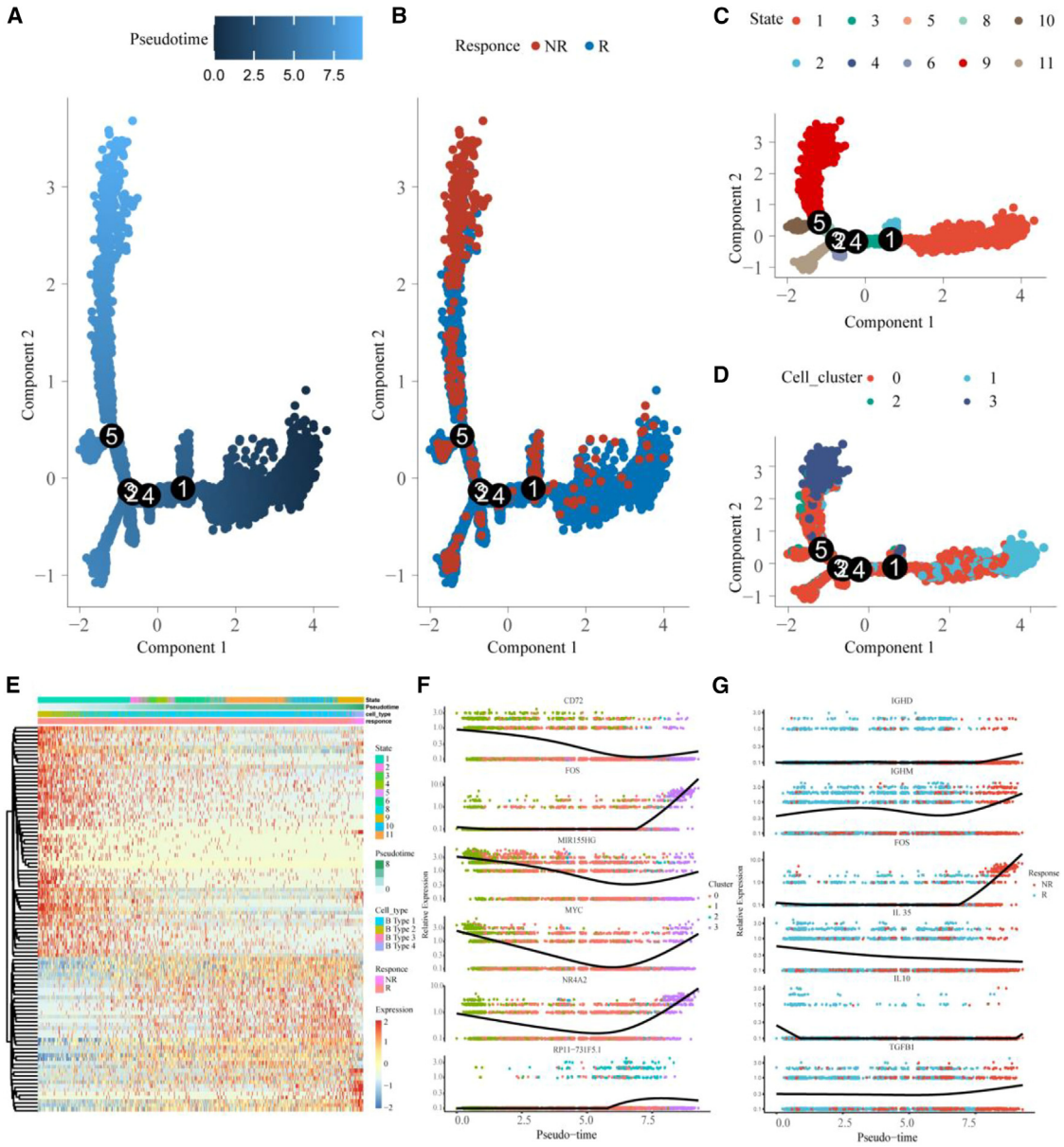

Figure 4. FOS⁺ B cells were in a mature state of differentiation

(A) The pseudotime analysis of B cells was exhibited, in which light blue represents more mature differentiation, while dark blue represents more naive cells. (B) The results of the pseudotime analysis of B cells in the R and NR groups show that B cells in the NR group are more mature. (C) The B cells were divided into 12 stages according to the results of the pseudotime analysis. (D) The results of the pseudotime analysis of four types of B cells show that the cells in the third and fourth groups are more mature. (E) This heatmap shows the relationship between cellular pseudotime score and cell stage, cell type, immunotherapy response, and gene expression. (F) Expression of differentially expressed genes in the third group of B cell differentiation. (G) Differential expression of B cell development-related genes and immune-negative genes during cell differentiation.

($p = 0.01$ for PFS, $p = 0.027$ for OS, Figures 7C and 7E). In an immunotherapy dataset (GSE179351) that included colorectal cancer ($n = 27$) and pancreatic cancer ($n = 17$), there was also a significant difference in efficacy between the high- and low-risk groups ($p = 0.01059$, Figure 6F). In validation set 1 (Figures S6A–S6C), which was also obtained by the fusion dataset mentioned above, there were significant differences in prognosis ($p = 0.016$) between patients in the high- and low-risk groups. We also validated the model in a uroepithelial cancer immunotherapy dataset ($n = 298$) with a 1-year OS predicted AUC of 0.68 and a 2-year OS predicted AUC of 0.8 (Figure S6D). Patients with low-risk scores all had better outcomes than those with high-risk scores ($p = 1.795 \times 10^{-4}$, Figure S6E). There

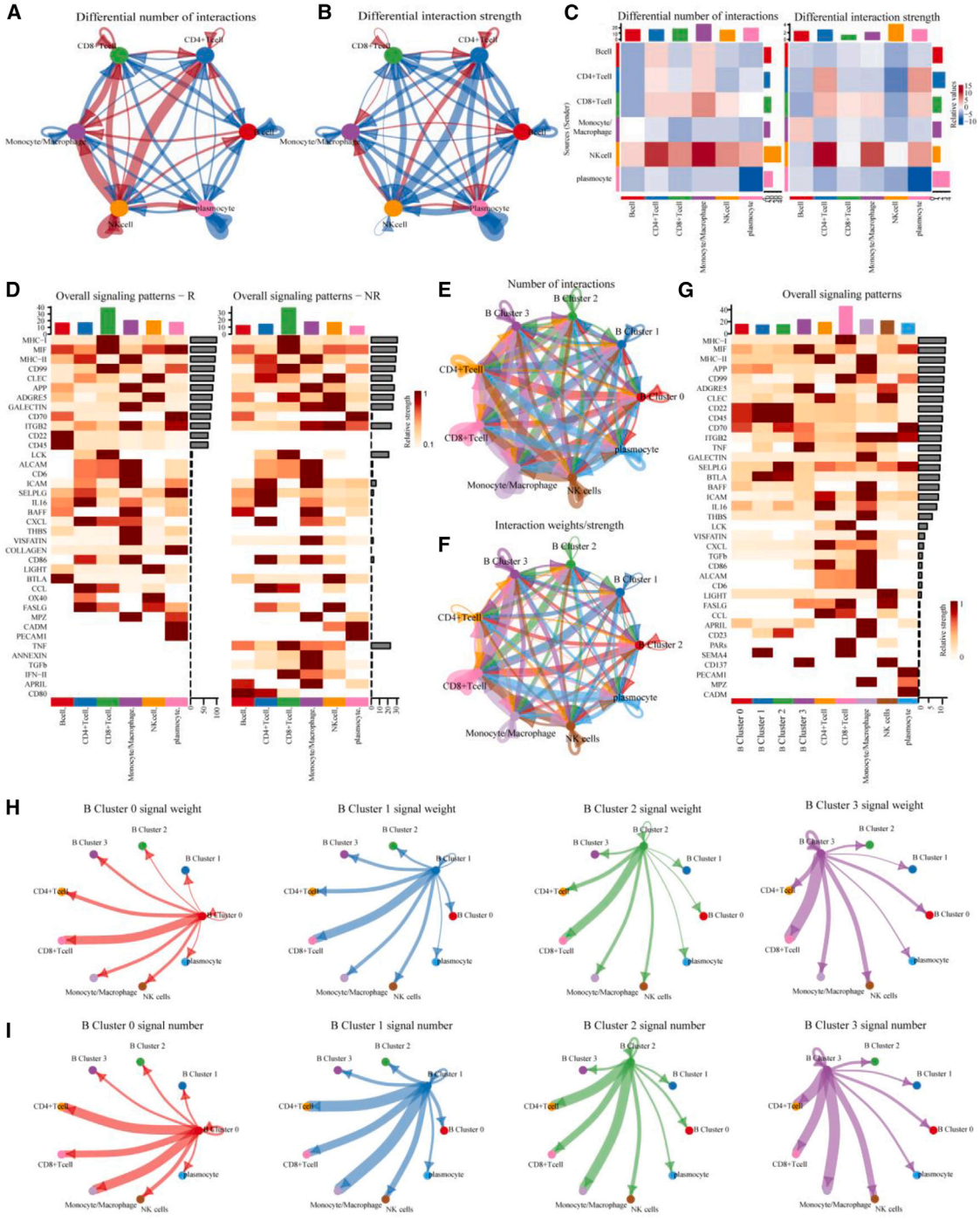

Figure 5. FOS$^+$ B cells can exert immunosuppressive effects on various immune cells

(A and B) Differences in the number and intensity of various interactions between immune cells in the NR group compared with the R group; blue color represents low number or weak intensity, arrows point to the cells receiving signals. (C) Heatmap of the number or intensity of differential signals. (D) Comparison of the expression of various intercellular signaling pathways between the R and NR groups. (E, F, H, and I) Intensity and number of interactions between immune cells after splitting B cells into four categories. (G) Expression of various cellular interaction pathways after splitting B cells into four categories.

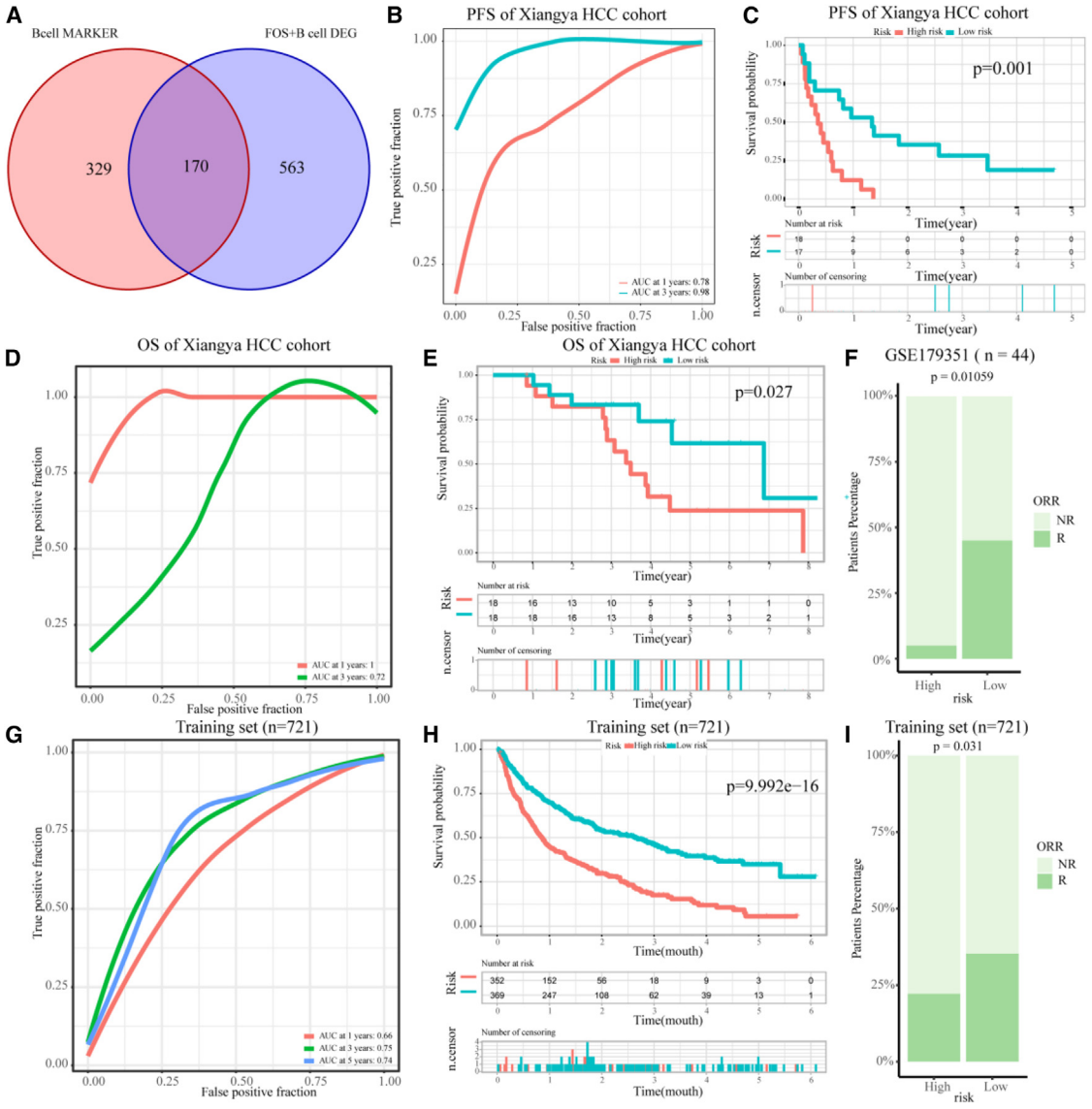

Figure 6. FOS⁺ B cell is reliable marker of immunotherapy efficacy and prognosis

(A) Intersection of 329 B cell marker genes and 563 differentially expressed genes in FOS⁺ B cells to obtain 170 genes. (B–E) The relationship between risk score and outcome in the Xiangya HCC immunotherapy cohort, and patients with high-risk scores had poorer PFS and OS. (F) The relationship between risk score and outcome in GSE179351, a colorectal cancer immunotherapy cohort. (G–I) The relationship between patient risk grouping and immunotherapy efficacy in the immunotherapy cohort of rectal or pancreatic cancer. HCC, hepatocellular carcinoma; OS, overall survival; PFS, progression-free survival.

was also a significant difference in efficacy between the high- and low-risk groups (p = 0.0015, Figure S6F). The above results also showed that FOS⁺ B cells are associated with immunotherapy resistance and a worse prognosis in pan-cancer.

FOS⁺ B cells negatively correlate with immunity status in pan-cancer patients

B cells play an important role in the tumor immune microenvironment, and we analyzed the relationship between FOS⁺ B cells and pan-cancer immune cells and the prognosis of pan-cancer patients using The Cancer Genome Atlas (TCGA) database. First, we analyzed the relationship of the FOS⁺ B cell risk score in pan-cancer with some immune function-related genes, including genes related to antigen presentation, cell adhesion, immune coactivation, immune co-inhibition, immune receptor, and immune ligand. We found that FOS⁺ B cells were largely negatively correlated with the expression of these genes (Figure 7A), suggesting that FOS⁺ B cells may suppress anti-tumor immunity. We then analyzed the infiltration of FOS⁺ B cells with various immune cells in the tumor microenvironment, and we found that FOS⁺ B cells also negatively correlated with the infiltration of

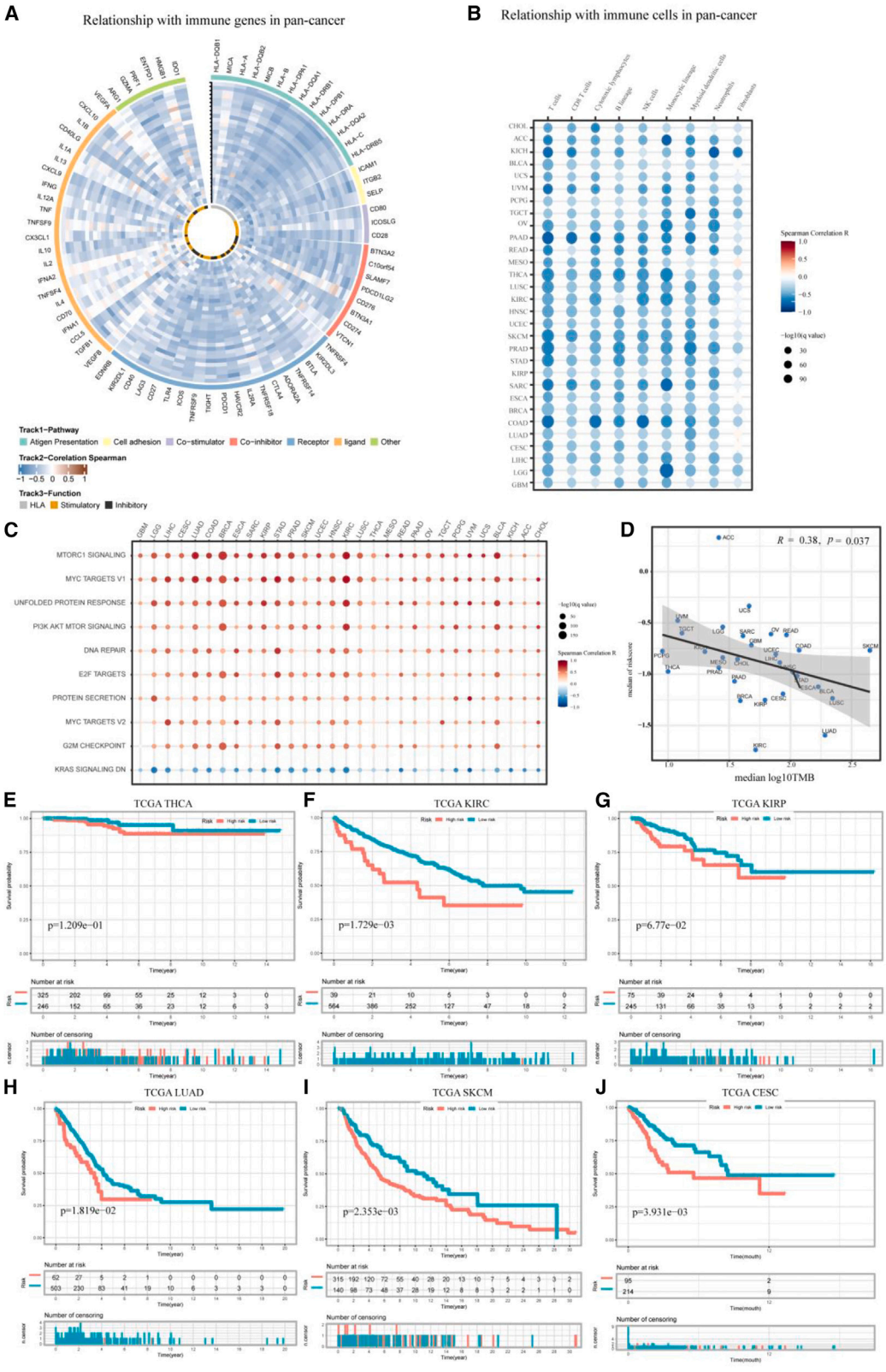

(legend on next page)

immune cells such as $CD8^+$ T cells, cytotoxic lymphocytes, and NK cells, which also supported their suppression of tumor immunity (Figure 7B). We also explored the relationship between FOS^+ B cells in pan-cancer and tumor marks (Hallmark), and the results showed that FOS^+ B cells positively correlated with these tumor markers and negatively correlated with the immunotherapy marker tumor mutation burden (TMB) (Figures 7C and 7D). To explore the relationship between FOS^+ B cells and the prognosis of patients with pan-cancer, we explored the relationship between FOS^+ B cell risk scores and patient prognosis in the TCGA database and found that FOS^+ B cell risk scores correlated with the prognosis of various tumors such as THCA, KIRC, KIRP, LUAD, and SKCM (Figures 7E–7J).

DISCUSSION

Immunotherapy has shown good effects in lung, esophageal, and colorectal cancer, but not all patients with malignancies benefit from immunotherapy,[20–22] and many patients develop primary or secondary drug resistance.[23,24] B cells, as an important role of immune cells, may have an important impact on the immunotherapy efficacy and prognosis of immunotherapy patients,[25,26] but the specific effects of different types of B cells on immunotherapy and their effect mechanisms are unclear. In this study, we used single-cell sequencing data from immunotherapy patients to classify B cells and found that FOS^+ B cells may reduce the efficacy of immunotherapy. Immunofluorescence analysis and pan-cancer immunotherapy cohort analysis also indicated that FOS^+ B cells negatively relate to immunotherapy efficiency and anti-tumor immunity.

In this study, we discovered that FOS^+ B cells were associated with the efficacy of immunotherapy in patients and may reduce the effect of immunotherapy. According to the National Center for Biotechnology Information (NCBI) GenBank, the FOS family includes members Fos, Fos-B, Fra1 (FOSL1), and Fra2 (FOSL2), which encode proteins containing a leucine zipper that can dimerize with the JUN family protein, such as JUNB.[27,28] The dimerization forms the activator protein 1 (AP1) complex and acts as a transcription factor (NCBI, 2020; Gene ID: 2353). Previous studies have shown that the Fos and c-fos genes are associated with proliferation, differentiation, transformation, and cell death.[29,30] The effect of Fos expression on tumor B cells has not been specifically investigated, but previous studies have shown that AP-1, composed of Fos and Jun, has an important effect on B cell differentiation and maturation.[31] Previous studies have revealed that the promoter of the Blimp1 gene contains AP-1 binding sites.[18] Blimp1 can promote the differentiation of B cells into antibody-secreting cells (ASCs), and c-Fos can bind to it to transactivate Blimp1 transcription, subsequently promoting the generation of ASCs. Therefore, we speculated whether AP-1 in B cells could promote Blimp1 and facilitate the differentiation of B cells into immunosuppressive plasma cells. However, due to the limited number of Blimp1-expressing cells in single-cell sequencing data, the correlation between JUNB, FOS, and Blimp1 was not particularly strong. Our research results also indicate that Blimp-1 levels were significantly increased in B cells of immunotherapy-resistant patients, and IgA expression was elevated in plasma cells. All these findings support our hypothesis, although further experimental verification is still required.

Prior studies have indicated an association between Bregs and a poor prognosis.[12] In addition, Bregs are known to secrete multiple immunosuppressive cytokines, including IL-10, IL-35, and TGF-β, suggesting their role in suppressing anti-tumor immunity, which could potentially diminish the efficacy of immunotherapy. In our current study, we also identified a subset of B cells characterized by FOS expression, indicating a relatively mature differentiation state. Notably, these FOS^+ B cells exhibited high levels of TGF-β expression but did not show elevated expression of IL-1. This suggests that, while the FOS^+ B cells identified in this study possess immunosuppressive properties like Bregs, their relationship with Bregs warrants further investigation. Some researchers have identified B cells with low CD21 expression in HIV-infected individuals, which are found in patients with long-term inflammatory responses. These $CD19^+CD10^-CD27^-CD21^{low}$ B cells may be associated with B cell exhaustion resulting from chronic inflammatory reactions.[32] However, in our study, FOS^+ B cells did not exhibit low CD21 expression, indicating that the FOS^+ B cells identified in our research do not align with this exhaustion B cell subtype. Therefore, we propose that FOS^+ B cells are not entirely synonymous with previously identified Bregs or exhaustion B cells but may represent a distinct subset of Bregs. Further research is needed to explore this possibility.

To further validate the relationship between FOS^+ B cells and immunotherapy efficacy and prognosis, we established a prognostic model of FOS^+ B cells and tested it in pan-cancer immune cell cohorts, including an HCC immunotherapy cohort from Xiangya Hospital. In all these cohorts, FOS^+ B cells were strongly associated with immunotherapy efficacy and prognosis. In the non-immunotherapy pan-cancer cohorts from TCGA, FOS^+ B cells were also associated with the prognosis of various tumors such as LUAD, THCA, SKCM, etc. FOS^+ B cells were negatively associated with immunophenotype-related genes such as antigen presentation and immune coactivation. Negative correlations with the degree of immune cell infiltration, such as $CD8^+$ T cells and cytotoxic lymphocytes, as well as with TMB, were also investigated. These results again suggest in the pan-cancer data that FOS^+ B cells may be negatively associated with immunotherapy efficacy and prognosis.

Figure 7. Association of FOS^+ B cells in pan-cancer with immunity and patient prognosis

(A) Association of FOS^+ B cell risk score with expression of multiple immune status-associated genes in pan-cancer. (B) Association of FOS^+ B cell risk score with the degree of infiltration of multiple immune cells in multiple cancers, with blue representing negative association. (C) Association of FOS^+ B cell risk score with multiple tumor markers, with red representing positive association and blue representing negative association. (D) Association of FOS^+ B cell risk scores with TMB in multiple cancers. (E–J) Prognostic differences between patients in high-risk and low-risk groups in multiple TCGA (The Cancer Genome Atlas) cohorts.

In this study, for the first time, we identified a subtype of B cells that is negatively associated with the efficacy of pan-cancer immunotherapy. Immunofluorescence analysis and pan-cancer immunotherapy cohort analysis also indicated that FOS^+ B cells negatively relate to immunotherapy efficiency and anti-tumor immunity. However, this study has the following shortcomings: first, although a large immunotherapy transcriptome cohort was used for analysis, the sample size of the single-cell dataset was still relatively small, which may cause some errors, and more cancer types should be integrated to characterize FOS^+ B cells. Second, the specific infiltration of FOS^+ B cells in NR patients and their interaction with other immune cells require further confirmation through basic research such as flow cytometry. Finally, Although AP-1 and JUNB in FOS^+ B cells can promote Blimp1 expression, Blimp1 is a pan-plasma cell marker and not specific to immunosuppressive plasma cells. This suggests that FOS^+ B cells may generate immunosuppressive plasma cells via alternative mechanisms beyond the AP-1/JUNB pathway. Further studies are needed to explore these potential mechanisms. Despite the above shortcomings, this study represents an important exploration of the correlation between B cells and immunotherapy efficacy and provides new ideas for further studies.

Conclusions

This study discovers and reports the correlation between FOS^+ B cells and immunotherapy resistance. This study provides evidence that FOS may form AP-1 with JUNB, thereby promoting the expression of Blimp-1 and subsequently facilitating the differentiation of B cells into immunosuppressive plasma cells. In addition, FOS^+ B cells may exert immunosuppressive effects on immune cells, including $CD8^+$ T cells, via the TNF signaling pathway.

MATERIALS AND METHODS

Publicly single-cell transcriptome and spatial transcriptome data

The scRNA-seq data of skin cancer, lung cancer, colon cancer, and HCC patients who received anti-PD-1 treatment were analyzed. The skin cancer data (GSE123813)[33] include a total of 40,314 immune cells from 10 patients with BCC, which was histologically confirmed. These 10 patients received 200 mg pembrolizumab every 3 weeks or 350 mg cemiplimab every 2 weeks. Six patients R, and 4 patients did NR.

The transcriptomic data of approximately 92,000 single cells from 12 patients with non-small cell lung cancer, who received neoadjuvant PD-1 blockade in combination with chemotherapy, are included in GSE207422.[34] Researchers assessed the treatment efficacy of these 12 patients using the RECIST1.1 criteria. Among these patients, 6 were evaluated as having a partial response, while the remaining 6 were assessed as having stable disease (SD). The publicly available single-cell data for immunotherapy patients is scarce, so we only identified and analyzed these two datasets from the GEO (Gene Expression Omnibus) database. We also conducted an analysis of a colorectal cancer spatial transcriptome dataset along with its corresponding single-cell transcriptome dataset (GSE144735).[35]

Xiangya single-cell transcriptome data

The single-cell data for immunotherapy patients with colon cancer and HCC used in this study were from Xiangya Hospital of Central South University. The study included single-cell data from two colon cancer patients who received immunotherapy, with one showing no response to the treatment and the other exhibiting a partial response. In addition, the study included single-cell data from an HCC patient who received immunotherapy and was evaluated as having SD following the treatment. The Medical Ethics Committee of Xiangya Hospital at Central South University approved the study protocol (ID: 2019050127), and patients provided informed consent.

For single-cell sequencing, patient surgical specimens were collected and wiped clean of surface fluids with lint-free paper. The tissues were then placed in 2 mL cryovials and stored at 2°C–8°C. The tissue was first transferred to a culture dish pre-filled with 1× PBS. Tissue pieces, measuring 0.5 mm^2, were cut and added to a dissociation solution (0.35% collagenase IV, 2 mg/mL papain, 120 units/mL DNase I). The reaction was carried out at 37°C in a shaking water bath at 100 rpm for 20 min. Subsequently, 1× PBS (containing 10% fetal bovine serum) was added to halt the dissociation process. The tissue pieces were then gently pipetted up and down 10 times using a pipette gun. The cell suspension was filtered through a 30-μm cell strainer. After that, the suspension was centrifuged at 300 × *g* for 5 min at 4°C, and the cell pellet was collected. The cell pellet was resuspended in 100 μL of 1× PBS (0.04% BSA) and then subjected to red blood cell lysis using 1 mL of red blood cell lysis buffer (MACS 130-094-183, 10×) for 2–10 min at room temperature. Following lysis, the cells were centrifuged at 300 × *g* for 5 min at room temperature, and the cell pellet was collected. Dead cells were removed using a dead cell removal kit (MACS 130-090-101). After the reaction, the cells were centrifuged to remove the reagent. The cells were then resuspended in 1× PBS (0.04% BSA) and centrifuged at 300 × *g* for 3 min at 4°C (repeated twice). This process resulted in a cell suspension containing candidate cells after tissue dissociation, red blood cell lysis, and dead cell removal. The cell suspension was then supplemented with 50 μL of 1× PBS (0.04% BSA). Cell viability was assessed using trypan blue staining, with a requirement of >85% cell viability. Cell counts were determined using a hemocytometer or an automated cell counter (Countess II Automated Cell Counter), with a cell concentration requirement of 700–1,200 cells/μL. The final cell suspension obtained after dissociation was loaded into the 10× Chromium instrument. Cell capture, cDNA amplification, and library construction were carried out according to the official kit instructions (10× Genomics Chromium Single-Cell 3′ kit, V3). After library construction, sequencing was performed on the NovaSeq 6000 sequencing platform (paired-end multiplexing run, 150 bp), with a sequencing depth requirement of 20,000 reads per cell.

Immunotherapy bulk RNA-seq data

To investigate the relationship and predictive role of FOS^+ B cells in immunotherapy efficacy, we systematically collected bulk RNA-seq

data and clinical information from patients across four ICI RNA-seq datasets. Three of the datasets were public datasets, while the HCC immunotherapy dataset was obtained from Xiangya Hospital of Central South University. The Xiangya HCC immunotherapy cohort is an immunotherapy bulk RNA-seq dataset collected from Xiangya Hospital of Central South University, which included RNA-seq data of 36 patients with HCC who received immunotherapy. The patients' surgical samples and clinical information were collected (Table S1). Secondary sequencing libraries were constructed by removing ribosomal RNA using the Human/Mouse/Rat Ribo-Zero rRNA Removal Kit (Epicenter, Madison, WI). At a high temperature, the poly(A)$^+$ or poly(A)$^-$ RNA fraction was cleaved into small fragments using divalent cations to ensure purification. We then constructed cDNA libraries using reverse transcription cleavage to obtain RNA fragments. The average insert size of a double-ended library is 250–350 bp. The cDNA libraries were sequenced on an Illumina NovaSeq 6000 system (LC-Bio Technology, Hangzhou, China) according to the recommended protocol.

One of the 3 publicly available datasets was downloaded from the GEO database (GSE179351),[36] which included transcriptomic data from 44 patients with colorectal or pancreatic cancer who received immunotherapy. The second publicly available dataset is IMvigor 210, which contains 298 patients with uroepithelial cancer who received immunotherapy.[37] The last publicly available dataset is a pan-cancer immunotherapy dataset obtained by fusing 10 public datasets as described by Zhang et al., who used the ComBat method to de-batch this fusion dataset.[38] We randomly divided this dataset into a training set (training set, n = 721) and a validation set (validation set 1, n = 154). In this study, the training set was used as a generalized cancer training set. Validation set 1, Imvigor 210, GSE179351, and the Xiangya dataset were used as validation sets to assess and validate the model.

Pan-cancer bulk RNA-seq data

The pan-cancer bulk RNA-seq data (TCGA) used in this study were obtained from the UCSC XENA data portal (https://xenabrowser.net).[39] Tumor mutation burden (TMB) data for tumor patients, used in this article for the analysis of the correlation between FOS$^+$ B cell downregulation and TMB, were obtained from the cBioPortal website (https://www.cbioportal.org).[40]

Single-cell transcriptome and spatial transcriptome analysis

We analyzed the scRNA-seq data using the R package "Seurat." To retain high-quality scRNA-seq data, the raw gene expression data for each cell was screened by applying 3 measures: only genes expressed in at least 5 single cells were used, cells expressing less than 100 genes were excluded, and cells with more than 5% of mitochondrial genes were removed.[41] To identify marker genes for each cell population, cutoff thresholds, adjusted p values <0.01, and log2 (fold change) of absolute values > 1 were used. For cluster annotation, we used some of the recognized marker genes of immune cells for annotation.[42] We evaluated cell-to-cell communication between different cell types using the "CellChat" package.[43] The R package "monocle2" was used for B cell differentiation pseudotime analysis.[44]

We analyzed spatial transcriptome data along with its corresponding single-cell sequencing data. Analysis of cell composition in the spatial transcriptome was performed based on gene expression in the single-cell data. The R package Seurat was employed to integrate the single-cell transcriptome and spatial transcriptome data.

Multiple immunofluorescence assays

The slides were initially treated with 4% paraformaldehyde for 15 min at room temperature, with gentle agitation, to fix the samples. Subsequently, for membrane protein labeling, they were permeabilized using 0.2% Triton X-100 for 10 min at room temperature. Following this, a 3% BSA solution was employed for blocking purposes, allowing for a 30-min incubation. Primary antibodies (CD20, 1:400; c-fos, 1:200; CDX2, 1:200) were applied and left to incubate overnight at 4°C. Subsequently, fluorescent secondary antibodies corresponding to the primary antibodies were incubated at room temperature for 1 h. Cell nuclei were labeled using DAPI. Immunofluorescence double-labeled cells were then collected and analyzed using a ZEISS confocal microscope.

Construction and validation of immunotherapy prediction model

FOS$^+$ B cell marker genes and B cell marker gene intersection were taken as FOS$^+$ B cell marker genes, and then we performed univariate Cox regression analysis to assess the cluster value of FOS$^+$ B cell marker genes on the OS of patients in the immunotherapy training set, and genes with $p < 0.01$ were identified as prognostic genes. Next, to minimize overfitting, prognostic genes were assessed by least absolute shrinkage and selection operator (LASSO) Cox proportional risk regression using the "glmnet" package. Based on the genes generated by the LASSO Cox regression analysis, we used multivariate Cox regression analysis to construct a risk prediction model and classified patients into low- or high-risk groups based on median cutoff values. To validate the predictive power of the model, we used the "survivalROC" package to calculate the AUC.[45] We used the R package "survminer"[46] and the Kaplan-Meier method for patient survival analysis. The log rank test was used to determine the statistical significance of the differences.

Pathway and functional enrichment analysis

We used the R package "clusterProfiler"[47] to perform gene ontology (GO) and functional enrichment analyses. GO analysis was performed using the enrichGO function of the R package "clusterProfiler," and GO annotations were based on the genome-wide annotation package (org.Hs.eg.db) released by the Bioconductor project.[48] The KEGG analysis was performed using the enrichKEGG function of the R package "clusterProfiler," which acquires pathway data and performs functional analysis through the latest online KEGG database.

Statistical analysis

We performed statistical analyses using R v.4.2.0 (https://www.r-project.org). We used Spearman correlation to assess the association between FOS$^+$ B cell risk scores and biological pathways or immune characteristics. The chi-square distribution was used to analyze differences in cell proportions. The Benjamini-Hochberg method was

used to calculate the false discovery rate, and the p value < 0.05 was considered significant.

DATA AND CODE AVAILABILITY

The data that support the findings of this study are available from the corresponding author upon reasonable request.

ACKNOWLEDGMENTS

This study was supported by grants from the National Natural Science Foundation of China (82403920, 82173342, 81874073, 81974384, and 62031023), the Reform and Development Fund for Colleges and Universities of Hunan Province (2050205), the Nature Science Foundation of Hunan Province (nos. 2021JJ31092, 2021JJ31048, and 2024JJ6662), the Science and Technology Innovation Program of Hunan Province (2024RC3042), the Youth Science Foundation of Xiangya Hospital (2023Q01), the Postdoctoral Fellowship Program of the CPSF under grant no. GZC20242044, the China Postdoctoral Science Foundation under grant no. 2024M753679, the Natural Science Foundation (Youth Fund) of Hunan Province of China (2022JJ40458), the Scientific Research Program of Hunan Provincial Health Commission (202203105261), the Fundamental Research Funds for the Central Universities of Central South University (2023ZZTS0023), the Nature Science Foundation of Changsha (kq2403008), and the Key Research and Development Program of Hainan Province (ZDYF2020228, ZDYF2020125 and ZDYF2022SHFZ087).

AUTHOR CONTRIBUTIONS

X.Z. and H.S. designed the study. X.Z., Y.Zhang, J.M., X.D., and Y.H. collected the data and performed the major analysis. J.T., S.Z., Y.Zhou, C.C., G.D., and Y.O. supervised the study. X.Z. and J.M. analyzed and interpreted the data. X.Z. and C.C. did the statistical analysis and drafted the manuscript. All authors read and approved the final manuscript.

DECLARATION OF INTERESTS

The authors declare no competing interests.

SUPPLEMENTAL INFORMATION

Supplemental information can be found online at https://doi.org/10.1016/j.omton.2024.200895.

REFERENCES

1. Zhou, F., Qiao, M., and Zhou, C. (2021). The cutting-edge progress of immune-checkpoint blockade in lung cancer. Cell. Mol. Immunol. *18*, 279–293.
2. Weng, J., Li, S., Zhu, Z., Liu, Q., Zhang, R., Yang, Y., and Li, X. (2022). Exploring immunotherapy in colorectal cancer. J. Hematol. Oncol. *15*, 95.
3. Shalhout, S.Z., Kaufman, H.L., Emerick, K.S., and Miller, D.M. (2022). Immunotherapy for Nonmelanoma Skin Cancer: Facts and Hopes. Clin. Cancer Res. *28*, 2211–2220.
4. Kalbasi, A., and Ribas, A. (2020). Tumour-intrinsic resistance to immune checkpoint blockade. Nat. Rev. Immunol. *20*, 25–39.
5. Van den Bossche, V., Zaryouh, H., Vara-Messler, M., Vignau, J., Machiels, J.P., Wouters, A., Schmitz, S., and Corbet, C. (2022). Microenvironment-driven intratumoral heterogeneity in head and neck cancers: clinical challenges and opportunities for precision medicine. Drug Resist. Updates *60*, 100806.
6. Bader, J.E., Voss, K., and Rathmell, J.C. (2020). Targeting Metabolism to Improve the Tumor Microenvironment for Cancer Immunotherapy. Mol. Cell *78*, 1019–1033.
7. Xu, L., Zou, C., Zhang, S., Chu, T.S.M., Zhang, Y., Chen, W., Zhao, C., Yang, L., Xu, Z., Dong, S., et al. (2022). Reshaping the systemic tumor immune environment (STIE) and tumor immune microenvironment (TIME) to enhance immunotherapy efficacy in solid tumors. J. Hematol. Oncol. *15*, 87.
8. Ugel, S., Canè, S., De Sanctis, F., and Bronte, V. (2021). Monocytes in the Tumor Microenvironment. Annu. Rev. Pathol. *16*, 93–122.
9. Downs-Canner, S.M., Meier, J., Vincent, B.G., and Serody, J.S. (2022). B Cell Function in the Tumor Microenvironment. Annu. Rev. Immunol. *40*, 169–193.
10. Kim, S.S., Sumner, W.A., Miyauchi, S., Cohen, E.E.W., Califano, J.A., and Sharabi, A.B. (2021). Role of B Cells in Responses to Checkpoint Blockade Immunotherapy and Overall Survival of Cancer Patients. Clin. Cancer Res. *27*, 6075–6082.
11. Fridman, W.H., Meylan, M., Petitprez, F., Sun, C.M., Italiano, A., and Sautès-Fridman, C. (2022). B cells and tertiary lymphoid structures as determinants of tumour immune contexture and clinical outcome. Nat. Rev. Clin. Oncol. *19*, 441–457.
12. Laumont, C.M., Banville, A.C., Gilardi, M., Hollern, D.P., and Nelson, B.H. (2022). Tumour-infiltrating B cells: immunological mechanisms, clinical impact and therapeutic opportunities. Nat. Rev. Cancer *22*, 414–430.
13. Ishigami, E., Sakakibara, M., Sakakibara, J., Masuda, T., Fujimoto, H., Hayama, S., Nagashima, T., Sangai, T., Nakagawa, A., Nakatani, Y., and Otsuka, M. (2019). Coexistence of regulatory B cells and regulatory T cells in tumor-infiltrating lymphocyte aggregates is a prognostic factor in patients with breast cancer. Breast Cancer *26*, 180–189.
14. Mao, Y., Wang, Y., Dong, L., Zhang, Q., Wang, C., Zhang, Y., Li, X., and Fu, Z. (2019). Circulating exosomes from esophageal squamous cell carcinoma mediate the generation of B10 and PD-1(high) Breg cells. Cancer Sci. *110*, 2700–2710.
15. Grün, D., and van Oudenaarden, A. (2015). Design and Analysis of Single-Cell Sequencing Experiments. Cell *163*, 799–810.
16. Lei, Y., Tang, R., Xu, J., Wang, W., Zhang, B., Liu, J., Yu, X., and Shi, S. (2021). Applications of single-cell sequencing in cancer research: progress and perspectives. J. Hematol. Oncol. *14*, 91.
17. Sarvaria, A., Madrigal, J.A., and Saudemont, A. (2017). B cell regulation in cancer and anti-tumor immunity. Cell. Mol. Immunol. *14*, 662–674.
18. Ohkubo, Y., Arima, M., Arguni, E., Okada, S., Yamashita, K., Asari, S., Obata, S., Sakamoto, A., Hatano, M., O-Wang, J., et al. (2005). A role for c-fos/activator protein 1 in B lymphocyte terminal differentiation. J. Immunol. *174*, 7703–7710.
19. Shalapour, S., Font-Burgada, J., Di Caro, G., Zhong, Z., Sanchez-Lopez, E., Dhar, D., Willimsky, G., Ammirante, M., Strasner, A., Hansel, D.E., et al. (2015). Immunosuppressive plasma cells impede T-cell-dependent immunogenic chemotherapy. Nature *521*, 94–98.
20. Steven, A., Fisher, S.A., and Robinson, B.W. (2016). Immunotherapy for lung cancer. Respirology *21*, 821–833.
21. Moehler, M., Högner, A., Wagner, A.D., Obermannova, R., Alsina, M., Thuss-Patience, P., van Laarhoven, H., and Smyth, E. (2022). Recent progress and current challenges of immunotherapy in advanced/metastatic esophagogastric adenocarcinoma. Eur. J. Cancer *176*, 13–29.
22. Zhao, W., Jin, L., Chen, P., Li, D., Gao, W., and Dong, G. (2022). Colorectal cancer immunotherapy-Recent progress and future directions. Cancer Lett. *545*, 215816.
23. Vesely, M.D., Zhang, T., and Chen, L. (2022). Resistance Mechanisms to Anti-PD Cancer Immunotherapy. Annu. Rev. Immunol. *40*, 45–74.
24. Sharma, P., Hu-Lieskovan, S., Wargo, J.A., and Ribas, A. (2017). Primary, Adaptive, and Acquired Resistance to Cancer Immunotherapy. Cell *168*, 707–723.
25. Ruffin, A.T., Cillo, A.R., Tabib, T., Liu, A., Onkar, S., Kunning, S.R., Lampenfeld, C., Atiya, H.I., Abecassis, I., Kürten, C.H.L., et al. (2021). B cell signatures and tertiary lymphoid structures contribute to outcome in head and neck squamous cell carcinoma. Nat. Commun. *12*, 3349.
26. Garaud, S., Dieu-Nosjean, M.C., and Willard-Gallo, K. (2022). T follicular helper and B cell crosstalk in tertiary lymphoid structures and cancer immunotherapy. Nat. Commun. *13*, 2259.
27. Liu, J., Nickolenko, J., and Sharp, F.R. (1994). Morphine induces c-fos and junB in striatum and nucleus accumbens via D1 and N-methyl-D-aspartate receptors. Proc. Natl. Acad. Sci. USA *91*, 8537–8541.
28. Karakaslar, E.O., Katiyar, N., Hasham, M., Youn, A., Sharma, S., Chung, C.H., Marches, R., Korstanje, R., Banchereau, J., and Ucar, D. (2023). Transcriptional activation of Jun and Fos members of the AP-1 complex is a conserved signature of immune aging that contributes to inflammaging. Aging Cell *22*, e13792.
29. Greenberg, M.E., and Ziff, E.B. (1984). Stimulation of 3T3 cells induces transcription of the c-fos proto-oncogene. Nature *311*, 433–438.
30. Cruz-Mendoza, F., Jauregui-Huerta, F., Aguilar-Delgadillo, A., García-Estrada, J., and Luquin, S. (2022). Immediate Early Gene c-fos in the Brain: Focus on Glial Cells. Brain Sci. *12*, 687.

31. Grötsch, B., Brachs, S., Lang, C., Luther, J., Derer, A., Schlötzer-Schrehardt, U., Bozec, A., Fillatreau, S., Berberich, I., Hobeika, E., et al. (2014). The AP-1 transcription factor Fra1 inhibits follicular B cell differentiation into plasma cells. J. Exp. Med. *211*, 2199–2212.

32. Roe, K. (2022). NK-cell exhaustion, B-cell exhaustion and T-cell exhaustion-the differences and similarities. Immunology *166*, 155–168.

33. Yost, K.E., Satpathy, A.T., Wells, D.K., Qi, Y., Wang, C., Kageyama, R., McNamara, K.L., Granja, J.M., Sarin, K.Y., Brown, R.A., et al. (2019). Clonal replacement of tumor-specific T cells following PD-1 blockade. Nat. Med. *25*, 1251–1259.

34. Hu, J., Zhang, L., Xia, H., Yan, Y., Zhu, X., Sun, F., Sun, L., Li, S., Li, D., Wang, J., et al. (2023). Tumor microenvironment remodeling after neoadjuvant immunotherapy in non-small cell lung cancer revealed by single-cell RNA sequencing. Genome Med. *15*, 14.

35. Lee, H.O., Hong, Y., Etlioglu, H.E., Cho, Y.B., Pomella, V., Van den Bosch, B., Vanhecke, J., Verbandt, S., Hong, H., Min, J.W., et al. (2020). Lineage-dependent gene expression programs influence the immune landscape of colorectal cancer. Nat. Genet. *52*, 594–603.

36. Parikh, A.R., Szabolcs, A., Allen, J.N., Clark, J.W., Wo, J.Y., Raabe, M., Thel, H., Hoyos, D., Mehta, A., Arshad, S., et al. (2021). Radiation therapy enhances immunotherapy response in microsatellite stable colorectal and pancreatic adenocarcinoma in a phase II trial. Nat. Can. (Ott.) *2*, 1124–1135.

37. Powles, T., Eder, J.P., Fine, G.D., Braiteh, F.S., Loriot, Y., Cruz, C., Bellmunt, J., Burris, H.A., Petrylak, D.P., Teng, S.L., et al. (2014). MPDL3280A (anti-PD-L1) treatment leads to clinical activity in metastatic bladder cancer. Nature *515*, 558–562.

38. Zhang, Z., Wang, Z.X., Chen, Y.X., Wu, H.X., Yin, L., Zhao, Q., Luo, H.Y., Zeng, Z.L., Qiu, M.Z., and Xu, R.H. (2022). Integrated analysis of single-cell and bulk RNA sequencing data reveals a pan-cancer stemness signature predicting immunotherapy response. Genome Med. *14*, 45.

39. Goldman, M.J., Craft, B., Hastie, M., Repečka, K., McDade, F., Kamath, A., Banerjee, A., Luo, Y., Rogers, D., Brooks, A.N., et al. (2020). Visualizing and interpreting cancer genomics data via the Xena platform. Nat. Biotechnol. *38*, 675–678.

40. Gao, J., Aksoy, B.A., Dogrusoz, U., Dresdner, G., Gross, B., Sumer, S.O., Sun, Y., Jacobsen, A., Sinha, R., Larsson, E., et al. (2013). Integrative analysis of complex cancer genomics and clinical profiles using the cBioPortal. Sci. Signal. *6*, pl1.

41. Song, P., Li, W., Guo, L., Ying, J., Gao, S., and He, J. (2022). Identification and Validation of a Novel Signature Based on NK Cell Marker Genes to Predict Prognosis and Immunotherapy Response in Lung Adenocarcinoma by Integrated Analysis of Single-Cell and Bulk RNA-Sequencing. Front. Immunol. *13*, 850745.

42. Paulson, K.G., Voillet, V., McAfee, M.S., Hunter, D.S., Wagener, F.D., Perdicchio, M., Valente, W.J., Koelle, S.J., Church, C.D., Vandeven, N., et al. (2018). Acquired cancer resistance to combination immunotherapy from transcriptional loss of class I HLA. Nat. Commun. *9*, 3868.

43. Jin, S., Guerrero-Juarez, C.F., Zhang, L., Chang, I., Ramos, R., Kuan, C.H., Myung, P., Plikus, M.V., and Nie, Q. (2021). Inference and analysis of cell-cell communication using CellChat. Nat. Commun. *12*, 1088.

44. He, Y., Chen, Q., Dai, J., Cui, Y., Zhang, C., Wen, X., Li, J., Xiao, Y., Peng, X., Liu, M., et al. (2021). Single-cell RNA-Seq reveals a highly coordinated transcriptional program in mouse germ cells during primordial follicle formation. Aging Cell *20*, e13424.

45. Heagerty, P.J., and Zheng, Y. (2005). Survival model predictive accuracy and ROC curves. Biometrics *61*, 92–105.

46. Wang, L., Wang, D., Yang, L., Zeng, X., Zhang, Q., Liu, G., and Pan, Y. (2022). Cuproptosis related genes associated with Jab1 shapes tumor microenvironment and pharmacological profile in nasopharyngeal carcinoma. Front. Immunol. *13*, 989286.

47. Yu, G., Wang, L.G., Han, Y., and He, Q.Y. (2012). clusterProfiler: an R package for comparing biological themes among gene clusters. OMICS *16*, 284–287.

48. Gentleman, R.C., Carey, V.J., Bates, D.M., Bolstad, B., Dettling, M., Dudoit, S., Ellis, B., Gautier, L., Ge, Y., Gentry, J., et al. (2004). Bioconductor: open software development for computational biology and bioinformatics. Genome Biol. *5*, R80.